SHAPE ANALYSIS OF THE 5' UNTRANSLATED REGION (UTR) OF MOUSE HEPATITIS VIRUS (MHV)

An Honors Fellows Thesis

by

FARYAL MASUD

Submitted to the Honors Programs Office
Texas A&M University
in partial fulfillment of the requirements for the designation as

HONORS UNDERGRADUATE RESEARCH FELLOW

April 2011

Majors: Biochemistry and Genetics

SHAPE ANALYSIS OF THE 5' UNTRANSLATED REGION (UTR) OF MOUSE HEPATITIS VIRUS (MHV)

An Honors Fellows Thesis

by

FARYAL MASUD

Submitted to the Honors Programs Office
Texas A&M University
in partial fulfillment of the requirements for the designation as

HONORS UNDERGRADUATE RESEARCH FELLOW

Approved by:

Research Advisor: Julian Leibowitz
Associate Director of the Honors Programs Office: Dave. A. Louis

April 2011

Majors: Biochemistry and Genetics

ABSTRACT

SHAPE Analysis of 5’ Untranslated Region of Mouse Hepatitis Virus.
(April 2011)

Faryal Masud
Department of Biochemistry and Biophysics
Texas A&M University

Research Advisors: Dr. Julian Leibowitz and Dr. Dong Yang
Department of Microbial and Molecular Pathogenesis

Software called SHAPE finder was used to analyze the secondary structure 5’ UTR of MHV. This study was the first time this software has been used for MHV, and if the previous procedures are followed, we will have high resolution results of the RNA secondary structures. Currently, the replication and pathogenesis of MHV is incompletely understood in part because of a lack of an accurate determination of its RNA secondary structure. This will help us better understand its course of proliferation. Since MHV is a good model for other coronaviruses and structures important for replication are most often conserved amongst closely related viruses, this information may provide a better understanding of the replication of related coronaviruses such as SARS-coronavirus.

DEDICATION

First of all, I dedicate this work to my dad who was not able to see this work to its completion. I could not have done it without his patience and support throughout this year.

I also dedicate this to all those close to me who I had to abandon for countless hours and countless weekends to work in the lab and on this thesis. It is a miracle I still have friends.

Finally, I dedicate this work to all young and growing scholars out there. It is possible to be inherently motivated about something that you are passionate about and to not give up, no matter the struggles you may encounter.

ACKNOWLEDGEMENTS

Thanks to Steven Silber for doing the NMR at the Texas A&M Department of Chemistry and for interpreting the results that showed we had our product necessary for modification.

Also, I would like to thank Dong Yang for letting me participate in this project which is part of her doctoral work, and Dr. Pinghua Liu for all of his help showing me the techniques necessary for these experiments, as well as helping me troubleshoot when problems were encountered throughout this entire project and before with previous projects.

Finally, I would like to thank Dr. Julian Leibowitz for allowing me to join his laboratory as an undergraduate and letting me use his resources which are not limited to his lab space and supplies but also his time and patience. I learned more and more about how to think like a scientist.

TABLE OF CONTENTS

Page

LIST OF FIGURES

LIST OF TABLES

CHAPTER I
INTRODUCTION

Mouse Hepatitis Virus (MHV) is a group two coronavirus of the Coronaviradae family in the order Nidovirales (6). It is a positive sense, single-stranded RNA virus that is 32 kb long. MHV provides a good animal model virus for a plethora of human diseases. The most recognized is Severe Acute Respiratory Syndrome (SARS) which is also caused by a coronavirus (18). A prerequisite for gaining an understanding of MHV pathogenesis is to study its means of replication. From previous studies, it is well known that the 5' untranslated region (UTR) of MHV contains cis-acting elements that are essential for viral replication (12, 14). The question that now arises is how this 5' UTR is involved in RNA-RNA interactions, RNA-protein interactions and other such important interactions that play a part in the replication and infection by the virus. In order to answer this question, a detailed understanding of the RNA secondary structures in this region of the virus must be identified.

Thus far, a proposed model for the first 140 nucleotides of the 5' UTR has been identified using phylogenetic evidence from nine other coronaviruses and other

---

This thesis follows the style of Journal of Virology

software such as Vienna RNA, Mfold and PKNOTS (10, 12, 20). These programs use tools such as free energy minimization for a given sequence, folding kinetics, and phylogenic evidence from RNA structures of related sequence families (2, 15-16). Vienna RNA in particular was utilized by Liu, et.al 2007 to examine the 5' UTR secondary structures of five group two coronaviruses, BCoV, human coronavirus HCoV-OC43, MHV-A59, HKU1, and SARS-CoV; three group one coronaviruses, HCoV-NL63, HCoV-229E, and TGEV and one group three coronavirus avian CoV IBV. Free energy minimization folding showed similar structures in the first 150 nt of the 5' UTR of three helical stems designated SL1, SL2, and SL4 (12). Of the group two viruses, two, HCoV-0C43 and SARS-CoV, were predicted to contain a fourth stem loop SL3. Figure 1 illustrates these structures. Although these are useful tools for identifying putative secondary structures, they are only 40-70% accurate (3). Most biochemical methods of determining RNA secondary structure can only be applied to short fragments of RNA. SHAPE, selective 2'-hydroxyl acylation analyzed by primer extension, is a new RNA analysis technique that can give the overall secondary structure at single nucleotide resolution for the entire genome (22). I will compare the secondary structure of the 5' UTR 140 nucleotide region, as determined by SHAPE, to that of the proposed model generated from phylogenetic evidence given by that of nine coronaviruses (12). As mentioned, all nine of the coronaviruses contain three stem loop secondary structures in their 5' UTR

despite having significant sequence differences and because of this, my hypothesis is that the 5’ UTR 140 nucleotide region will contain these three stem loop structures as well.

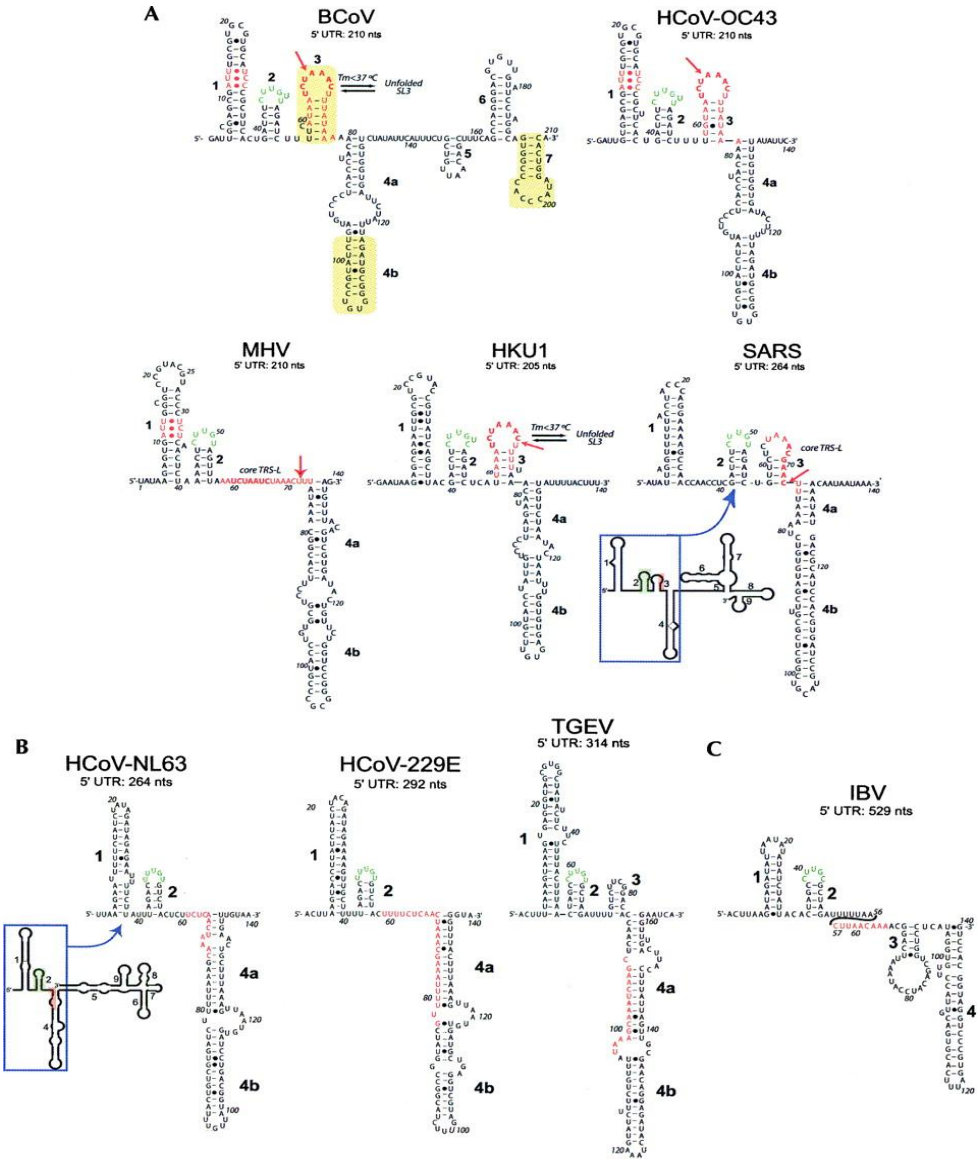

FIG 1. Models of 5’ UTR of nine coronaviruses. From Liu, et al. 2007, this figure is a good illustration of the predicted models of the 5’ UTR of the nine coronaviruses discussed.

The mechanism by which SHAPE works involves a chemical reaction between an electrophile, in this case 1-methyl-7-nitroisatoic anhydride (1M7), and flexible RNA nucleotides containing the ribose 2' hydroxyl group that all RNAs have (17, 23). These flexible RNA nucleotides must be exposed to sufficient concentrations of 1M7 to yield at least one 2'- O adduct per 300 nucleotides (23). After formation of these adducts, primers are annealed to the template to generate cDNA using reverse transcription. The adducts are detected by their ability to block the reverse transcription process (23). The control in this experiment is a separate RNA that is run without the use of 1M7 to subtract background (23). The cDNAs are finally resolved by electrophoresis, typically on a sequencing/genetic analyzer, and quantified nucleotide by nucleotide eliminating background. Higher band intensity is correlated with high reactivity. High reactivity indicates a region of unpaired nucleotides whereas a region of low intensity indicates the presence of secondary structures. SHAPE has thus far not been applied to MHV. Before getting to this thorough analysis of the virus, a standard must be used to test the primer extension and SHAPE software. We will be using pUC-18 cDNA standard and four primers each with a different fluorescence label to test the reaction.

SHAPE has been applied to determine the RNA secondary structures of other viruses such as HIV-1 (23). They used a method applying SHAPE to four

different states of the virus including the in virio state meaning recovering virus genome from inside the native HIV virus, the ex virio state meaning the HIV genome deproteinized and extracted from the virus capsid, an in vitro transcript of HIV, and a slightly modified in viro virus with disrupted interactions between the capsid and RNA. For our study with MHV, we will be focusing on two of these relevant states, the in virio and ex virio states for the 5' 950 nt of the 5' UTR and part of the coding region, nsp1. The first 474 nts of this region contains cis-acting sequences required for replication. Nsp1 is a 28 kilodalton gene that generates one of the first processed proteins of the virus and is believed to have a crucial role in the early life cycle MHV (1, 4). In another study, SHAPE was used to identify the secondary structures in the entire HIV-1 genome (22). They discovered that noncoding regions, such at the UTR in MHV, have many more secondary structures than the coding regions of the virus. My hypothesis for this 950 nt region is that those sequences in the 5' UTR will be more highly structured than that of the coding nsp1 region based on this study by Watts et. al 2009.

The electropherograms generated from SHAPE experiments provide much structural information that must then be analyzed with significantly complex algorithmic steps to generate quantitative data. Vasa, et al. 2008 developed a set of tools called ShapeFinder to more quickly analyze the raw electropherograms

without complex steps. These simplifications using this software tool include converting fluorescence intensity to quantitative cDNA concentrations, correcting for signal decay, and aligning reactivity data to the known RNA sequence (21). Therefore, we will be using Shapefinder to analyze our data generated by SHAPE reactions.

If all of this holds true, the next part of the experiment would be to determine the presence of secondary structures determined by SHAPE using the reverse genetic approach. In previous experiments, both biochemical and reverse genetic approaches have been used to determine structure of the 3' UTR of MHV and test proposed models. The biochemical approach is prevalent in earlier works of the 3' UTR. The Masters lab in 2000 added to a proposed structure of the 3' UTR by showing that a previously identified bulged stem loop consisting of five bulges actually had larger terminal and internal loops than previously thought (7-8). In 2001, the Leibowitz lab illustrated by disrupting base pairing that several essential stem loops that make up two host protein binding elements exist in the last 166 nt of the 3' UTR using DI RNA replication (13). The reverse genetic approach was then utilized by Goebel, et al. in 2004. This involves making point mutations in the viral sequence to test the viability of the virus which is then measured by viral ability to infect cells (5). This approach is known to be successful and has been

applied to a model of the 3’ UTR and tested by Johnson, et al. in 2005 (9). These same tests can be applied to the 5’ UTR. It is clear that knowledge of the 5’ UTR secondary structure of MHV and its interactions with other proteins and RNAs is vital to understanding its means of proliferation and has applications in developing treatments.

CHAPTER II
METHODS

Virus production

Virus and cell media

17CL-1 cells were grown with Dulbecco's modified Eagle medium (Life Technologies) supplemented with 10% fetal bovine serum, 4 mM glutamine and penicillin/streptomycin. Trypsin was used to passage cells. MHV-A59 was propagated in 17CL-1 cells as previously described (11). The virus was clarified of cellular debris with centrifugation following a previous, successful protocol (11).

Molecular cloning of A fragment of MHV

Bacterial media

LB broth and 100 µg/mL ampicillin was used to grow *E. coli* containing the plasmids. pLitmus 38 and the A plasmid from the MHV reverse genetic system (24-25).

Minipreps

The Qiagen miniprep kit and protocol were used. Cells were centrifuged at 5000 rpm for 2 minutes in microcentrifuge tubes, the supernatant decanted leaving the

cell pellet. The pellet was dissolved in buffer P1 + RNase A by vortexing. Cells were lysed by the addition of buffer P2 lysis solution with gentle mixing. Neutralization buffer N3 was added and mixed gently and the lysed bacteria centrifuged at 12,000 rpm for 10 minutes. Supernatant was added to a QIAprep column in a 2 mL collection tube, centrifuged for 30 seconds and additional supernatant was added to the column and centrifuged a second time. Columns were washed with buffer PE and dried by centrifugation. QIAprep columns were placed in new collection tubes and eluted DNA with buffer EB (10 mM Tris-HCl, pH 8.5). We stored samples at -20° C.

Agarose gel electrophoresis

Agarose gels (0.8%) buffered with 1X TAE and contained ethidium bromide as the DNA staining agent. Samples contained 6X DNA dye and a 1kb DNA ladder was used as marker. Electrophoresis was for 45 min at 120V. Gels were photographed under UV light.

PCR

PCR reactions were assembled using 5 PRIME Master Mix, forward and reverse primers, and plasmid samples. (See Table 1 for PCR primer sequences). PCR was carried out as follows: 1 cycle 96° C 1 min, 30 cycles of 96° C 30 sec, 60° C 30 sec, 72° C 2 min, 1 cycle 72° C 15 min, hold at 4° C.

Gel purification

After agarose gel electrophoresis, the desired fragment was excised with a scalpel and the DNA extracted from the gel and purified using the Qiagen gel purification kit according to the Vendors instructions. Briefly, gel slices were weighed and added appropriate volumes of buffer to solubilize the gel. Incubated at 50° C for 10 min. Isopropanol was added to the sample and bound to the DNA binding column. Washed with buffer PE, and eluted with water.

Quantification

DNA was quantified by UV spectrophotometry using a Nanodrop Spectrophotometer.

Restriction Digest

Spe I and Mlu I was utilized from NEB along with appropriate buffers for digestion of A fragment and. pLitmus 38.

Ligation

Purified pLitmus 38 and A fragments were taken to create a ligation reaction using T4 DNA ligase and buffer.

Transformation

Top 10 electrocompetent cells were used in electroporation. With ligation product and cells, electroporated 1 time at 2.5 kV with a time constant of 4.64. To

the mixture SOC media was added and put in shaker at 37° C for 1 hour. Spread onto LB amp plates.

Plate counting

Picked eight colonies and put into LB amp media and shook over night at 37° C.

Sequencing reaction

Big-Dye mix, miniprep template, water, forward primer in one, reverse primer in the other was added to PCR tubes. (See Table 2 for sequencing primer sequences) Sequencing program: 1 cycle 96° C 2 min, 35 cycles of 96° C 20 sec, 50° C 10 sec, 60° C 4 min, hold at 4° C.

Labeling and modification

Synthesis of 1M7

The detailed procedure for the synthesis of 1M7 was generously given to us by the Kevin Weeks laboratory. 4NIA was dissolved in 60mL of DMF and added to NaH in 15mL DMF, stirring in a flame dried round bottom flask under N_2 gas. A bright cloudy orange solution resulted at first which turns clear orange after a few minutes. 1.5 g of dissolved MeI was added dropwise and stirred at room temperature for four hours. The reaction was poured into 100 mL cold 1M HCl and the resulting orange precipitate collected by vacuum filtration, washed with

ice cold water and then with ether. The 1M7 was dried overnight in a vaccum oven in a watch glass. The final product yield should be around 79% and is a bright orange powdery solid. NMR was completed with the following specs: 1H NMR (CO(CD3)2, 400 MHz) 3.69 (s, 3H, -NCH3-), 8.12 (dd, J=8.8 Hz, 2 Hz, 1 H, ArH), 8.2 (d, J=2hz, 1h, ArH), 8.34 (d, J=8.4 Hz, 1 H, ArH).

Creating primers

Four good primers were selected in terms of GC content, minimal ability to form dimers or hairpins, and melting temperature sites closest to the 5' end of the pUC-18 standard and ordered from Eurofins. One good priming site for MHV-A59 was also selected. The results were four primers of that would yield products of size 186, 219, 237, and 273. The MHV primer is in positions 261-282. (See Table 2 for primer sequences.)

Labeling primers

We purchased the fluorescence dyes JOE, TAMARA, FAM and ROX through ANASPECT and used the Invitrogen labeling protocol (19). The oligonucleotide was dissolved in deionized water, extracted three times with chloroform and then precipitated with 3 M NaCl and ethanol. After mixing well and incubating at –80° C for 30 minutes the solution was centrifuged at ~12,000 × *g* for 30 minutes. The supernatant was removed; the pellet was rinsed twice with cold 70% ethanol and dried under vacuum. The dry pellet is dissolved in deionized water to achieve a

final concentration of 25 μg/μL and stored at –20° C. A 0.1 M sodium tetraborate buffer was prepared by dissolving 0.038 g of sodium tetraborate decahydrate per mL of waterand the pH adjusted with HCl to 8.5. This tetraborate labeling buffer was prepared as close as possible to the time of labeling. We dissolved 250 μg of the amine-reactive compound in 14 μL DMSO. For FAM and TAMRA succinimidyl ester, we used 200 μg for100 μg of oligonucleotide and allowed the compound to equilibrate to room temperature before opening. The material was dissolved by pipetting and washing the sides of the vial. To the vial containing the reactive label in DMSO, we added: deionized water, labeling buffer, oligonucleotide stock solution. The reaction was incubated for at least six hours or overnight at room temperature placing the vial on a shaker oscillating at low speed, gently vortexing to mix the vial every half hour for the first two hours to ensure that the reaction remained well mixed. After six hours, 50–90% of the amine-modified oligonucleotide molecules are labeled. The labeled oligonucleotide was precipitated by adding3 M NaCl and cold 100% ethanol to the vial, mixing well and incubating at –20° C for 30 minutes. The precipitated labeled oligonucleotide was recovered by centrifugation at ~12,000 × g for 30 minutes. We removed the supernatant, rinsed the pellet once or twice with cold 70% ethanol, and dried briefly.

Purifying the Labeled Oligonucleotide by Gel Electrophoresis (19)

To purify the labeled oligonucleotide by gel electrophoresis, we poured a 20%

polyacrylamide gel, resuspended the pellet from ethanol precipitation in 50% formamide, and incubated at 55° C for 5 minutes. The oligonucleotide was loaded onto the gel and also loaded an adjacent well with 50% formamide plus 0.05% bromophenol blue. Electrophoresis was performed until the bromophenol blue indicator dye was two-thirds of the way down the gel. We removed the gel from the glass plates, placed it on Saran Wrap, and laid it on a fluorescent TLC plate. The labeled and unlabeled oligonucleotides were located by illuminating with a UV source. The band containing the labeled oligonucleotide was cut out with a scalpel and the oligonucleotide eluted by the chopping it into pieces and incubating overnight on a rotator in 4° C.

Creating standard

A culture of *E. coli* containing pUC-18 was grown overnight in LB containing ampicillin at 37° C. The culture was inoculated into a larger flask of LB amp and grown at 37°C over night. Plasmid DNA was extracted using the Omega Plasmid MidiKit. Plasmid was quantified with a Nanodrop spectrophotometer to determine how much enzyme to digest it with. Restriction digests with BamHI or PstI were performed in the appropriate NEB buffer at 37° C over night. Restriction digestion was monitored by agarose gel. When the digestion was complete, we proceeded to add chloroform and NaOAc, followed by centrifugation for two minutes and transfer of the top layer into a new 1.5 mL tube and precipitating the digested DNA by the addition of 100% ethanol. After

incubating at -80° C for 1-4 hours the DNA was pelleted by centrifugation for 10 minutes. The supernatant was discarded and pellets washed in 100% ethanol and recovered by centrifugation for 5 minutes. Alcohol was poured off and the pellet dried for 20 minutes and dissolved in water. We next digested the samples with AatII in NEB buffer 3 and an appropriate volume of water over night at 37° C. The sample was electrophoresed in an agarose gel with the entire sample and performed a gel extraction with Qiagen kit to retrieve the smaller fragment of pUC-18 that we needed for testing our primers in a SHAPE reaction.

The following is a summary of the proposed experiment design for this project and follows the procedures done by Watts et. al in 2009 when using SHAPE to study the secondary structures in HIV-1:

1. Virus Production: MHV-A59 strain that I will be working will infect 17CL-1 cells. At 72 hours after the infection, viruses will be purified from culture supernatants by low speed centrifugation to remove cellular debris followed by ultracentrifugation through a sucrose pad and resuspended in MOPS buffer, pH 6.6, containing monovalent and divalent ions that are consistent with maintaining the RNA secondary structure. RNA will be quantified by quantitative reverse-transcription PCR. Half of the sample will be frozen at -80°C to be used as the in virio state while the remaining aliquot will be used as the ex virio state.

2. RNA modification: Treat the ex virio aliquot with subtilisin (an agent used to remove proteins from the RNA). Subdivide this sample again into that treated with 1M7 and that which will remain untreated. The same procedure should be mimicked for the frozen in virio sample without subtilisin treatment. This RNA should then be purified using a prepared kit.
3. Primer extension: The necessary primers will be annealed to the template of both the modified and the control RNA. This will allow the production of cDNA in a reverse transcription reaction.
4. Capillary electrophoresis and data processing: Instead of running a sequencing gel, capillary electrophoresis on an ABI 3130 sequencing instrument can resolve the cDNA. Shapefinder software can use the raw electrograms to generate data based on fluorescence intensity on a nucleotide by nucleotide resolution level.
5. Reverse genetic approach: If novel unforeseen secondary structures are elucidated, then this method will be used to discover the functional role of these structures. This involves piecing together an entire cDNA fragment of MHV containing the 5' UTR and creating mutants that have a mutation in the novel secondary structure that are predicted to disrupt function if the structure is important to function. This should be compared to the wild type MHV. From here the viral RNA transcript is electroporated into the desired cell line and the cultures are observed microscopically over 3 days to search for

evidence of virus replication. A plaque assay is performed after this to determine the effectiveness of the virus at replicating. These plaques will finally be picked, amplified in cell culture, and reverse transcribed and sequenced to see the final sequence of the virus recovered. I have conducted previous studies using the reverse genetic approach for the 3' UTR and completed a manuscript for this data that will soon be published.

TABLE 1. Forward and reverse PCR primers

PCR Primers	Sequence
Forward	GCGACTAGTTATAAGAGTGATTGGCGTCCG
Reverse	CGTACGCGTAAAGGGCCTTGGAGGTAGTCACTCTAGTT GAGGCCTCCACCTTCTGGGGATCCTCATCTAC

TABLE 2. Sequencing primers

Sequencing Primer	Sequence
26-47 afrag	GTAGTTTAAATCTAATCTAATC
282-261 afrag	GGGTTACCCAACTTCTCCGATG

TABLE 3. Single stranded amplification primers

Primer	Sequence
pUC 18-273	CAGAGCAGATTGTACTGAGAG
pUC 18-237	GTGAAATACCGCACAGATGC
pUC 18-219	GCGTAAGGAGAAAATACCGCATC
pUC 18-186	CGCCATTCAGGCTGCGCAACTG
A59 (-) -282-261	ATGCGTTCGGAAGCATCCATGG

CHAPTER III
RESULTS

Virus production

A small scale comparison of virus yield from 17CL1 cells or DBT demonstrated that 17CL1 cells produced 2-5 times more virus than DBT cells. Thus far 19 L of virus has been produced by infection of 17CL1 cells. This virus has thus been clarified of cellular debris and is being stored in the -80°C freezer.

Benchtop SHAPE experiment

Following the Weeks protocol, an orange-colored powder was created that was to be used in our modification reactions. The first time, the powder was determined by NMR to only be about 30% of the desired product (1M7). In a second synthesis, the powder was determined to be 70% of the desired product. The product is stored in a vacuum desiccator over desiccant at room temperature. The following is the H-NMR spectrum of the final product.

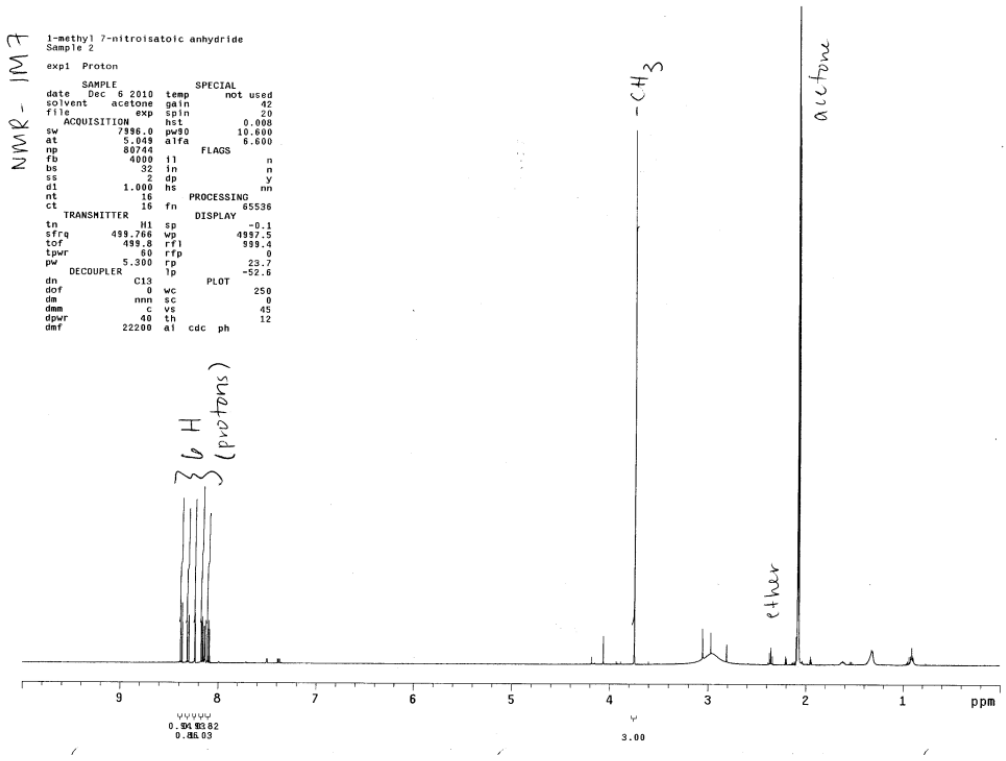

FIG 2. 1H-NMR spectrum of 1M7 product. The sample was solubilized in deuterated acetone. There is some residual ether from washing the product. The 6 H proton spikes indicate the presence of the desired product.

Molecular cloning of A fragment

Molecular cloning was a success. I created clones of the plasmid containing the A fragment in pLitmus 38. Six out of the eight colonies were the correct size of 3.2 kb (2.7 + 500 bp of vector and A); however only one had the correct sequence when confirmed with a sequencing reaction.

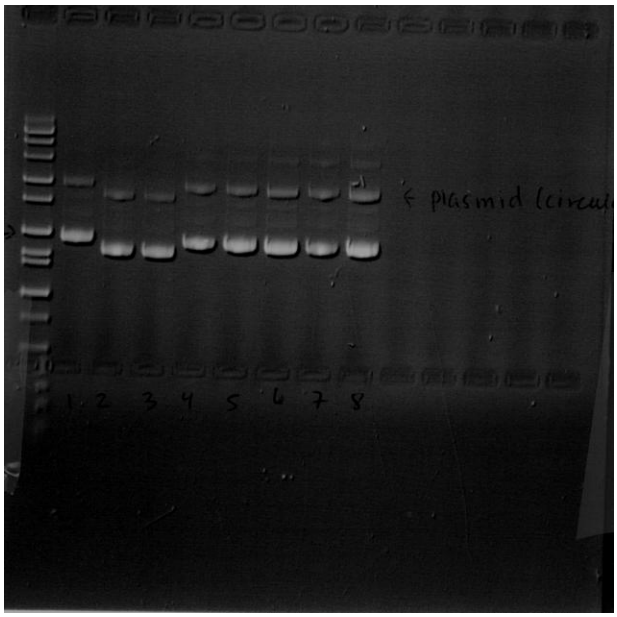

FIG 3. pLitmus 38 with A insert. Marked lanes 1, 4-8 appear to have the correct insert from the size of the fragment (excluding marker lane). When sent for sequencing, only the sample in lane 5 had the desired sequence.

Labeling primers with fluorescent dyes

Primers from Table 3 were successfully labeled following the protocol using JOE, ROX, TAMARA, and FAM nearing 90-100% efficiency. The following is a sample calculation of labeling efficiency:

For JOE, the spectrophotometer gave us an absorbance of 1.137 at 260 nm and 0.3535 at 520 nanometers. The correction factor given to us by the company for JOE was .25. The extinction coefficients at 260 and 520 were 75,000 and 200,3000 respectively.

$$A\ (260\ nm) = 1.137 - 0.3535 * (.25) = 1.0453$$

$$\frac{[dye]}{[DNA]} = \frac{0.3535}{75{,}000} * \left(\frac{200{,}300}{1.0453}\right) * 100\% = 90.3\%$$

To test the accuracy of the spectrophotometer, we used the Nanodrop data:

$$A(260) = \ 0.105 - 0.033 * (.25) = 0.09675$$

$$\frac{[dye]}{[DNA]} = \frac{0.033}{75{,}000} * \left(\frac{200{,}300}{0.09675}\right) * 100\% = 91.1\%$$

The results were similar enough that we could trust either instrument to give us the correct labeling efficiency. Table 4 outlines all of the dye efficiencies.

TABLE 4. Efficiency of labeling

Dye	Efficiency using spectrophotometer:	Efficiency using Nanodrop:
JOE-237	96%	102%
JOE-viral (282-261)	90%	92%
TAMARA-219	108%	104%
TAMARA-viral (282-261)	95%	95%
ROX-186	106%	107%
ROX- viral (282-261)	107%	115%
FAM-273	126%	109%
FAM- viral (282-261)	102%	100%

Single stranded amplification of pUC 18 fragment

pUC 18 was successfully purified and digested with BamH I; this template however, lead to nonspecific priming when single stranded amplification was attempted despite several attempts with different PCR conditions as seen in Figure 4.

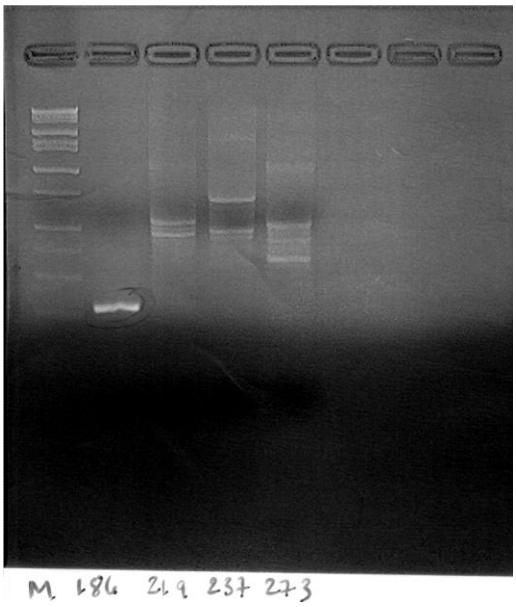

FIG 4. Nonspecific priming in single stranded amplification. Lane 1-marker. Lane 2-186 fragment shows the correct size fragment without nonspecific priming. Lanes 3-4 show multiple bands indicative of nonspecific priming.

The template was then digested with Bam H I and and Aat II to create a smaller fragment in an attempt to eliminate nonspecific priming. After adjusting conditions with gradient PCR, I was able to get the desired fragments as seen in

Figure 5. However, when these samples were sent to be run on the electropherogram, the results were inconclusive.

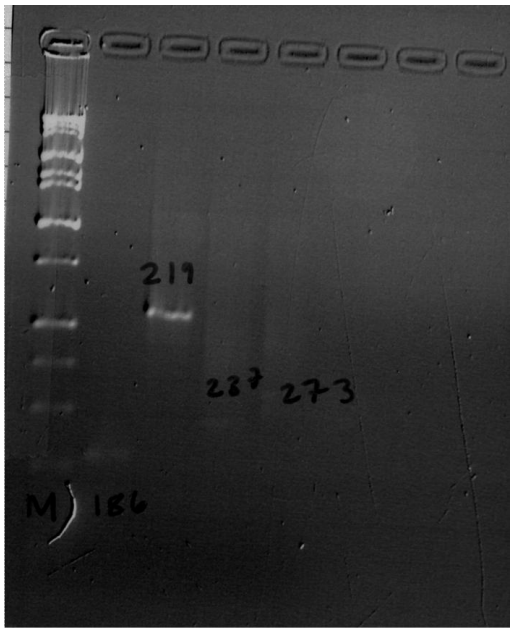

FIG 5. Single stranded amplification. Lane 1-marker. Lane 2-186 bp fragment. Lane 3-one fragment however the size is incorrect being the size of the whole template about 500 bp. Lane 4-237 bp fragment. Lane 5-273 bp fragment.

CHAPTER IV
DISCUSSION AND CONCLUSIONS

There are several reasons as to why the standards may not have been read by the electropherogram to give us our raw standard data. After running a gel purification with the entire single stranded amplification product, it is possible that much of the product was lost in the purification process as the original bands visible on the gel were very faint indication low concentration. In previous runs, fragments of that size were known to appear faint because of their small size so the experiment was continued in an attempt to get a baseline for our viral experiments. In our next approach, I will amplify up to ten reactions instead of five and pool the products before purification. As of now, the 237 bp fragment has yet to primed and amplified and I have only been able to amplify the entire template. I will attempt to get a standard from pLitmus 38 to replace this fragment, and label its primer. This primer is sure to generate the desired fragment as it has previously been used for sequencing.

The currently ongoing step is labeling the A-59 primer that will be used in primer extension to create viral cDNA. After we obtain a standard we will linearize the viral DNA with Mlu I, gel purify it and perform in vitro transcription to generate RNA. The next step will be to run a PAGE gel in order to get the desired 500 bp

segment that we need. We will then purify the RNA purify and set up a reverse transcription reaction to generate cDNA. Finally we will sequence with the electropherograms. One sample will be modified with 1M7 and the other will not be modified as outlined in the methods. These sample data can finally be input into ShapeFinder which will automatically subtract the standard and we will be able to view the secondary structures in the 5’ UTR.

REFERENCES

1. **Brockway, S. M., and M. R. Denison.** 2005. Mutagenesis of the murine hepatitis virus nsp1-coding region identifies residues important for protein processing, viral RNA synthesis, and viral replication. Virology **340:**209-223.

2. **Chen, S. J., and K. A. Dill.** 2000. RNA folding energy landscapes. Proc Nat Acad Sci **106:**97-102.

3. **Deigan, K. E., T. W. Li, D. H. Mathews, and K. M. Weeks.** 2009. Accurate SHAPE-directed RNA structure determination. Proc Natl Acad Sci USA **106:**97-102.

4. **Denison, M. R., and S. Perlman.** 1987. Identification of purative polymerase gene product in cells infected with murine coronavirus A59. Virology **157:**565-568.

5. **Goebel, S. J., B. Hsue, T. F. Dombrowski, and P. S. Masters.** 2004. Characterization of the RNA components of a putative molecular switch in the 3' untranslated region of the murine coronavirus genome. J Virol **78:**669-682.

6. **Gorbalenya, A. E., L. Enjuanes, J. Ziebuhr, and E. J. Snijder.** 2006. Nidovirales: evolving the largest RNA virus genome. Virus Res. **117:**17-37. Epub 2006 Feb 2028.

7. **Hsue, B., T. Hartshorne, and P. S. Masters.** 2000. Characterization of an essential RNA secondary structure in the 3' untranslated region of the murine coronavirus genome. J. Virol. **74:**6911-6921.

8. **Hsue, B., and P. S. Masters.** 1997. A bulged stem-loop structure in the 3' untranslated region of the genome of the coronavirus mouse hepatitis virus is essential for replication. J Virol **71:**7567-7578.

9. **Johnson, R. F., M. Feng, P. Liu, J. J. Millership, B. Yount, R. S. Baric, and J. L. Leibowitz.** 2005. Effect of mutations in the mouse hepatitis virus 3'(+)42 protein binding element on RNA replication. J Virol. **79:**14570-14585.

10. **Kang, H., M. Feng, M. E. Schroeder, D. P. Giedroc, and J. L. Leibowitz.** 2006. Putative cis-acting stem-loops in the 5' untranslated region of the severe acute respiratory syndrome coronavirus can substitute for their mouse hepatitis virus counterparts. J Virol. **80:**10600-10614.

11. **Kim, K. H., K. Narayanan, and S. Makino.** 1997. Assembled coronavirus from complementation of two defective interfering RNAs. J Virol **71:**3922-3931.

12. **Liu, P., L. Li, J. J. Millership, H. Kang, J. L. Leibowitz, and D. P. Giedroc.** 2007. A U-turn motif-containing stem-loop in the coronavirus 5' untranslated region plays a functional role in replication. RNA **13:**763-780.

13. **Liu, Q., R. F. Johnson, and J. L. Leibowitz.** 2001. Secondary structural elements within the 3' untranslated region of mouse hepatitis virus strain JHM genomic RNA. J Virol **75:**12105-12113.

14. **Liu, Y., E. Wimmer, and A. V. Paul.** 2009. Cis-acting RNA elements in human and animal plus-strand RNA viruses. Biochem Biophys Acta **1789:**495-517.

15. **Mathews, D. H., M. D. Disney, J. L. Childs, S. J. Schroeder, M. Zuker, and D. H. Turner.** 2004. Incorporating chemical modification constraints into a dynamic programming algorithm for prediction of RNA secondary structure. Proc Natl Acad Sci USA **101:**7287-7292. Epub 2004 May 7283.

16. **Mathews, D. H., J. Sabrina, M. Zuker, and D. H. Turner.** 1999. Expanded sequence dependence of thermodynamic parameters improves prediction of RNA secondary structure. J Mol Biol **288:**911-940.

17. **Merino, E., Wilkinson, K., Coughlan, J., and Weeks, K.** 2005. RNA structure analysis at single nucleotide resolution by selective 2'-hydroxyl acylation and primer extension (SHAPE). Journal of American Chemical Society **127:**4223-4231.

18. **Rota, P. A., M. S. Oberste, S. S. Monroe, W. A. Nix, R. Campagnoli, J. P. Icenogle, S. Penaranda, B. Bankamp, K. Maher, M. H. Chen, S. Tong, A.**

Tamin, L. Lowe, M. Frace, J. L. DeRisi, Q. Chen, D. Wang, D. D. Erdman, T. C. Peret, C. Burns, T. G. Ksiazek, P. E. Rollin, A. Sanchez, S. Liffick, B. Holloway, J. Limor, K. McCaustland, M. Olsen-Rasmussen, R. Fouchier, S. Gunther, A. D. Osterhaus, C. Drosten, M. A. Pallansch, L. J. Anderson, and W. J. Bellini. 2003. Characterization of a novel coronavirus associated with severe acute respiratory syndrome. Science **300:**1394-1399.

19. **Sambrook, J., E. F. Fritsch, and T. Maniatis.** 1989. Molecular cloning: a laboratory manual, Second Edition. Cold Spring Harbor Laboratory, New York.

20. **Schroeder, S. J.** 2009. Advances in RNA structure prediction from sequence: new tools for generating hypotheses about viral RNA structure-function relationships. J Virol **83:**6326-6334.

21. **Vasa, S. M., N. Guex, K. A. Wilkinson, K. M. Weeks, and M. C. Giddings.** 2008. ShapeFinder: a software system for high-throughtput quantitative analysis of nucleic acid reactivity information resolved by capillary electrophoresis. RNA **14:**1979-1990.

22. **Watts, J. M., K. K. Dang, R. J. Gorelick, C. W. Leonard, J. W. Bess, Jr., R. Swanstrom, C. L. Burch, and K. M. Weeks.** 2009. Architecture and secondary structure of an entire HIV-1 RNA genome. Nature **460:**711-716.

23. **Wilkinson, K. A., R. J. Gorelick, S. M. Vasa, N. Guex, A. Rein, D. H. Mathews, M. C. Giddings, and K. M. Weeks.** 2008. High-throughput SHAPE analysis reveals structures in HIV-1 genomic RNA strongly conserved across distinct biological states. PLoS Biol **6:**883-899.

24. **Yount, B., K. M. Curtis, E. A. Fritz, L. E. Hensley, P. B. Jahrling, E. Prentice, M. R. Denison, T. W. Geisbert, and R. S. Baric.** 2003. Reverse genetics with a full-length infectious cDNA of severe acute respiratory syndrome coronavirus. Proc Natl Acad Sci USA **100:**12995-13000.

25. **Yount, B., M. R. Denison, S. R. Weiss, and R. S. Baric.** 2002. Systematic assembly of a full-length infectious cDNA of mouse hepatitis virus strain A59. J. Virol. **76:**11065-11078.

CONTACT INFORMATION

Name:	Faryal Masud
Professional Address:	c/o Dr. Julian Leibowitz Department of MMPA 232 SRPH Texas A&M Health Science Center College Station, TX 77843
Email Address:	faryalmasud@gmail.com
Education:	B.S., Biochemistry and Genetics Texas A&M University, May 2011 Magna Cum Laude Undergraduate Research Fellow